CELL DEATH FOLLOWING THERMAL NEUTRON EXPOSURE

L.C. Paterson[1*], J. Atanackovic[2], C. Boyer[3], S. El-Jaby[1], N.D. Priest[1], C.B. Seymour[4], D.R. Boreham[4], R.B. Richardson[1]
[1]Atomic Energy of Canada Limited
([*]paterslc@aecl.ca)
[2]Ontario Power Generation, [3]Canadian Neutron Beam Centre,
[4]McMaster University

Abstract

When individuals are exposed to unknown external ionizing radiation, it is desirable to have the means to assess both the absorbed dose received (Gy) and the radiation quality. Yet, conventional biodosimetry techniques, specifically the dicentric chromosome assay, cannot differentiate between the damage caused by high- and low-linear energy transfer (LET) exposures. Frequencies of apoptosis and necrosis, may provide an alternative method that assesses both the absorbed dose and radiation quality after unknown exposures. For this preliminary study, human lymphocytes were irradiated with ^{60}Co gamma rays and thermal neutrons. Both apoptosis and necrosis increased with increasing gamma dose. In contrast, no dose-response was observed following thermal neutron exposure at doses up to 2.61 Gy.

1. Introduction

Thermal neutrons present an occupational radiation hazard to nuclear energy workers (NEWs) in a variety of facilities including research and power reactors. Understanding the mechanisms by which thermal neutrons interact with tissue is a necessary precursor for determining potential health effects. To date, there is little experimental data that describes the cellular effects of thermal neutron exposure and no published data specifically pertaining to cell death, the latter being a common endpoint used in quantitative assessments of absorbed radiation dose. Cell death can be achieved via a variety of pathways including apoptosis, necrosis, senescence, autophagocytosis, and mitotic catastrophe. In this paper, preliminary data relating to apoptosis and necrosis following thermal neutron exposures are presented.

Apoptosis, first described in 1972 by Kerr et al. [1], is a highly regulated and conserved form of cell death identified by easily-observed and tightly-regulated morphological changes. It is also the main mode of cell death in lymphocytes following exposure to gamma radiation [2, 3]. In this process, phosphatidylserine (PS) transfer from the inner cell membrane to the outer cell membrane is a highly conserved characteristic that is observed in all organisms. The presence of PS on the external cell membrane aids in recruiting macrophages [4] and presents an excellent binding site for Annexin V-labeling which is commonly employed for apoptotic cell detection. Apoptotic cell death does not produce an associated inflammatory response and, as such, the resulting biological consequences are less disruptive to normal tissue function than necrotic cell death. In contrast, necrosis is often described as either an unregulated or accidental form of cell death whereby the cell breaks apart, spilling its contents into the surrounding tissue. However, recent evidence has indicated that the process may sometimes be under genetic control and that biochemical cascades mediate the necrotic response [5]. While much work is still required to

understand necrotic regulation, the endpoint of cellular rupture creates an inflammatory response that has the potential to induce tumorigenesis [6].

Previous studies have established direct correlations between damage to lymphocytes and absorbed dose following whole- and partial-body exposures to low- and high-LET radiations. This holds true for a variety of endpoints including chromosome aberrations and apoptosis [7-15]. Currently, though, there is no data describing correlations between the cell death mechanisms of apoptosis and necrosis in lymphocytes following thermal neutron exposure. Studies have examined lymphocyte exposure to 280 keV neutrons [13] and 14.5 MeV neutrons [7] and determined that regardless of energy, the relative biological effectiveness (RBE) for apoptotic cell death is approximately unity. Similar apoptotic RBE values of 1.3 to 3.0 have been found following lymphocyte exposure to high energy nitrogen nuclei with kinetic energies ranging between 32 to 45 MeV [16]. With this said, it is also accepted that RBE values vary with biological endpoint. For instance, significantly higher RBE values for thermal neutrons have been observed using the dicentric chromosome assay (DCA) – the currently accepted gold-standard biodosimetry technique. Cytogenetic data using the DCA indicate that thermal neutrons have a high RBE of 36.4 ± 13.3 [11].

It has been theorized that cells respond differently to densely ionizing radiation in contrast to less densely ionizing radiation. Specifically, densely ionizing, high LET radiation types are expected to produce significantly more DNA double-strand breaks (DSB) per cell hit in contrast to low-LET radiation types [17]. Following radiation-induced DSBs, cells may correctly repair the damage, mis-repair the damage that may ultimately result in mutations, or undergo cell death. This work aims to provide a better understanding of lymphocyte cell death, specifically apoptosis and necrosis, following thermal neutron exposure

2. Methodology

Three healthy male volunteer blood donors, ages 25 to 65, participated in this study. Though all donors were included in the cell death portion of this study, only a single donor was used for the assessment of chromosome aberrations. The DCA was performed to verify that cell damage is occurring following thermal neutron exposure. Whole blood from the donors was first drawn by venipuncture into either sodium heparin (for gamma irradiations) or sodium citrate (for neutron irradiations) vacutainers (BD Biosciences). Aliquots of 1.5 mL of blood were then immediately transferred into 15 mL polypropylene test tubes for irradiation. The choice of anticoagulant was varied from sodium heparin to sodium citrate for neutron exposures to eliminate the undue influence of the additional nitrogen content found in sodium heparin.

2.1 Neutron and Gamma Irradiation Geometries and Dose Determination

Thermal neutron irradiations were performed at the National Research Universal (NRU) reactor in collaboration with the Canadian Neutron Beam Centre (CNBC). Specifically, 15 mL polypropylene test tubes, each containing 1.5 mL of blood, were suspended in front of the N5 Triple-Axis Spectrometer beam port that was adjusted to a beam dimension of 1” × 2” (Figure 1). The thermal neutron doses delivered ranged between 0.03 Gy and 2.6 Gy using a dose rate of 2.33 Gy h^{-1} (see Table 1 for doses delivered). Three control tubes were set-up to ensure that

extraneous factors did not affect our results. The laboratory control blood tubes remained in the cell culture laboratory throughout the sample irradiation. The NRU control was taken to the reactor, but not placed near the neutron beam or in the gamma field. The gamma field control was placed in the resulting gamma field directly below the neutron beam port.

Table 1: Thermal neutron dose and irradiation timings.

Thermal Neutron Dose (Gy)	Irradiation Time (s)
0.000	--
0.04	53
0.09	134
0.17	269
0.26	403
0.35	538
0.87	1344
1.74	2689
2.61	4043

The neutron dose delivered to the blood volumes was indirectly determined using the Monte Carlo N-Particle (MCNP 5) radiation transport code [18]. In these simulations, the neutron beam and target geometry illustrated in Figure 1 was modeled. The composition of blood was input using elemental compositions given in ICRP Publication 23 [19]. The thermal neutron fluence rate at the sample holder was calculated to be 2.80×10^{8} neutrons cm^{-2} s^{-1}. Fluence to kerma conversion coefficient for thermal neutrons, which in this particular situation is equivalent to dose absorbed, was calculated to be 2.31×10^{-13} Gy cm^{2}. This neutron kerma factor is well aligned with published values [11, 20]

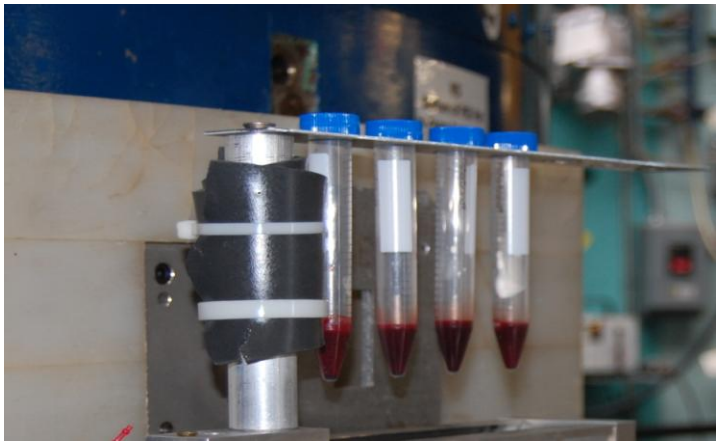

Figure 1: Thermal neutron irradiation set-up.

The relevant neutron interactions following thermal neutron blood irradiation are summarized in Table 2. Due to the irradiation geometry, and specifically the dimensions of the test tube, it was determined that dose delivered to the blood was predominantly a result of the $^{14}N(n,p)^{14}C$ reaction. This (n,p) reaction yields a proton with an energy of 590 keV [21]. In water, the proton will have a range of approximately 10.8 μm [22]. As blood is approximately 80% water [23], it can be assumed that a similar proton range will be observed. The gamma rays are of minimal

consequence due to their range in water being much greater than the dimensions of the test tube and therefore they are lost from the system.

Table 2: Relevant neutron interactions following blood irradiation.

Reaction	Cross Section (b) ($1\ b = 1.0 \times 10^{-24}\ cm^2$)	Blood Composition (% by weight)	Natural Abundance (%)	Half-life ($t_{1/2}$)
$^{1}H(n,\gamma)^{2}H$	0.33	10.0	99.9	
$^{14}N(n,p)^{14}C$	1.83	2.91	99.9	5715 years
$^{35}Cl(n,\gamma)^{36}Cl$	43.6	0.27	75.8	3.01×10^{5} years

Gamma irradiation was completed using AECL's ^{60}Co GammaCell 200 and GammaCell 220 irradiators. ^{60}Co has a half-life of 5.27 years and decays to ^{60}Ni via beta decay. During this decay, two mono-energetic gamma rays with energies of 1.17 MeV and 1.33 MeV are emitted. Doses from the ^{60}Co sources ranged from 0.03 Gy to 2.5 Gy. The dose rate ranged from 4.57 Gy h^{-1} to 4.75 Gy h^{-1} for the low dose samples and 214 Gy h^{-1} to 222 Gy h^{-1} for samples receiving 0.63 Gy and higher (Table 3). The dose rate variation is due to the time between irradiations and the decay of ^{60}Co.

Table 3: Gamma doses and dose rates.

^{60}Co Gamma Dose (Gy)	Dose Rate (Gy h^{-1})
0.00	--
0.03	4.57 – 4.75
0.06	4.57 – 4.75
0.13	4.57 – 4.75
0.19	4.57 – 4.75
0.25	4.57 – 4.75
0.63	214 – 222
1.25	214 – 222
1.88	214 – 222
2.50	214 – 222

2.2 Cell Assays

Immediately following irradiation, lymphocytes were isolated using Ficoll Paque PLUS (GE Health Care) and cell cultures were prepared containing 9 mL of Roswell Park Memorial Institute RPMI-1640 medium (Hyclone), 15% fetal bovine serum (Sigma-Aldrich), 100 units mL^{-1} penicillin and 100 μg mL^{-1} streptomycin (Sigma-Aldrich). Cultures were incubated for 48 hours at 37 °C with 5% CO_2 in air.

2.2.1 Dicentric Chromosome Assay

As described elsewhere [24], for chromosome cultures, 1% phytohemagglutinin type M (PHA-M) (Gibco) and 15 μM 5-bromo-2'-deoxyuridine (BrdU) (Sigma-Aldrich) were added. 0.1 μg mL^{-1} of Colcemid (Gibco) was added for the final four hours to arrest cells in metaphase. To harvest, cells were treated with 75 mM KCl and washed three times with Carnoy's Fixative (3 parts methanol: 1 part glacial acetic acid). Slides were made using the Hanabi Metaphase Spreader (Transition Technologies Inc.). Fluorescence-Plus-Giemsa (FPG) staining was achieved by immersing the slide in 20 μg mL^{-1} Bisbenzimide H 33258 for 2 minutes, exposing

the slide to UV light for 4 minutes followed by 10 minutes in 10% Giemsa Stain. Complete metaphase spreads were analysed for dicentric and ring chromosomes.

2.2.2 Apoptosis and Necrosis Cell Death Assays

For the cell death assays, following the 48 hour incubation, cells were washed in phosphate buffered saline (Hyclone) and 100 µL of suspension was transferred to a 1.7 mL tube for flow cytometry. 10 µL of Annexin V-FITC and 20 µL of 7-aminoactinomycin D (7AAD) (both Beckman Coulter) were added to the cell suspension. Flow cytometry was completed using an ImageStream (AMNIS Corp.) and its associated Inspire™ (AMNIS Corp.) software. The 488 nm laser was used for excitation of Annexin V-FITC and 7AAD. Fluorescent, bright-field, and side-scatter images were captured together with compensation controls for each fluor. Data analysis was performed using the Ideas™ (AMNIS Corp.) software package. Image data was gated to ensure only single cells were analysed. Up to 20,000 cells were captured per donor per dose.

3. Results

3.1 Cell Death Assays

When the intensity of Annexin V-FITC is plotted against the intensity of 7AAD, four populations may be distinguished (Figure 2). Cells expressing both low Annexin and low 7AAD are considered live, undamaged cells, while cells expressing low Annexin but high 7AAD are referred to as live, damaged cells. High Annexin, low 7AAD cells are considered to be early apoptotic cells. It is now widely accepted that the high Annexin, high 7AAD populations are composed of both traditional necrotic cells and late-apoptotic cells (also called secondary necrosis).

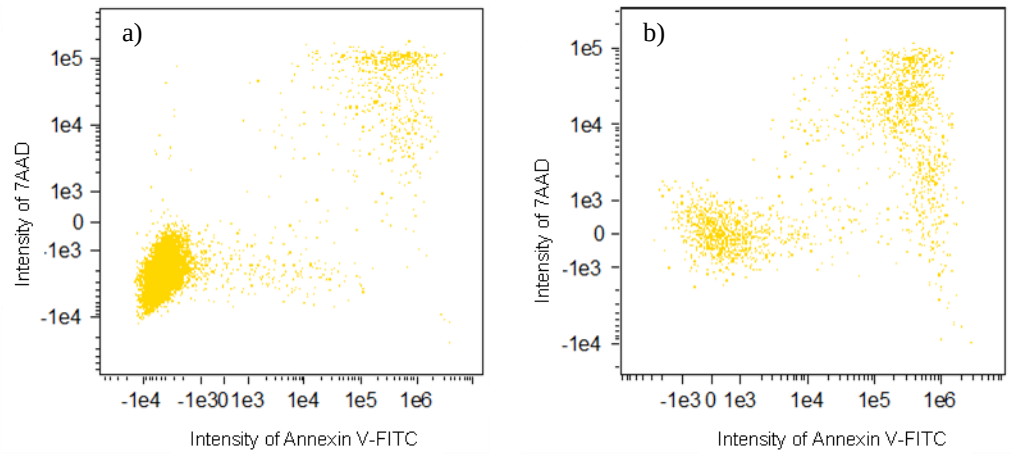

Figure 2: Cell death response following 1.741 Gy of thermal neutron radiation (a) and 1.875 Gy Gamma (b). The intensity of Annexin V-FITC versus 7AAD for Donor 3 is shown.

Secondary necrosis is a result of apoptotic cell death *in vitro* – this process is not normally observed *in vivo* where phagocytic cells take up apoptotic cells prior to self-degradation (which results in plasma membrane breakdown, and provides a mechanism for 7AAD entry) [25]. Using the AMNIS ImageStream, it is possible to distinguish between primary and secondary necrosis based on morphological appearance, however this data has not been included in this paper.

Figure 3 illustrates percent cell death as a function of absorbed dose. Following gamma exposure, both apoptosis and necrosis show an upwards trend with dose (R^2 of 0.90 and 0.59, respectively). However, thermal neutron data for both apoptosis and necrosis maintains a flat profile, with no demonstrated relationship to dose (ie. R^2 values of 0.02 and 0.04, respectively).

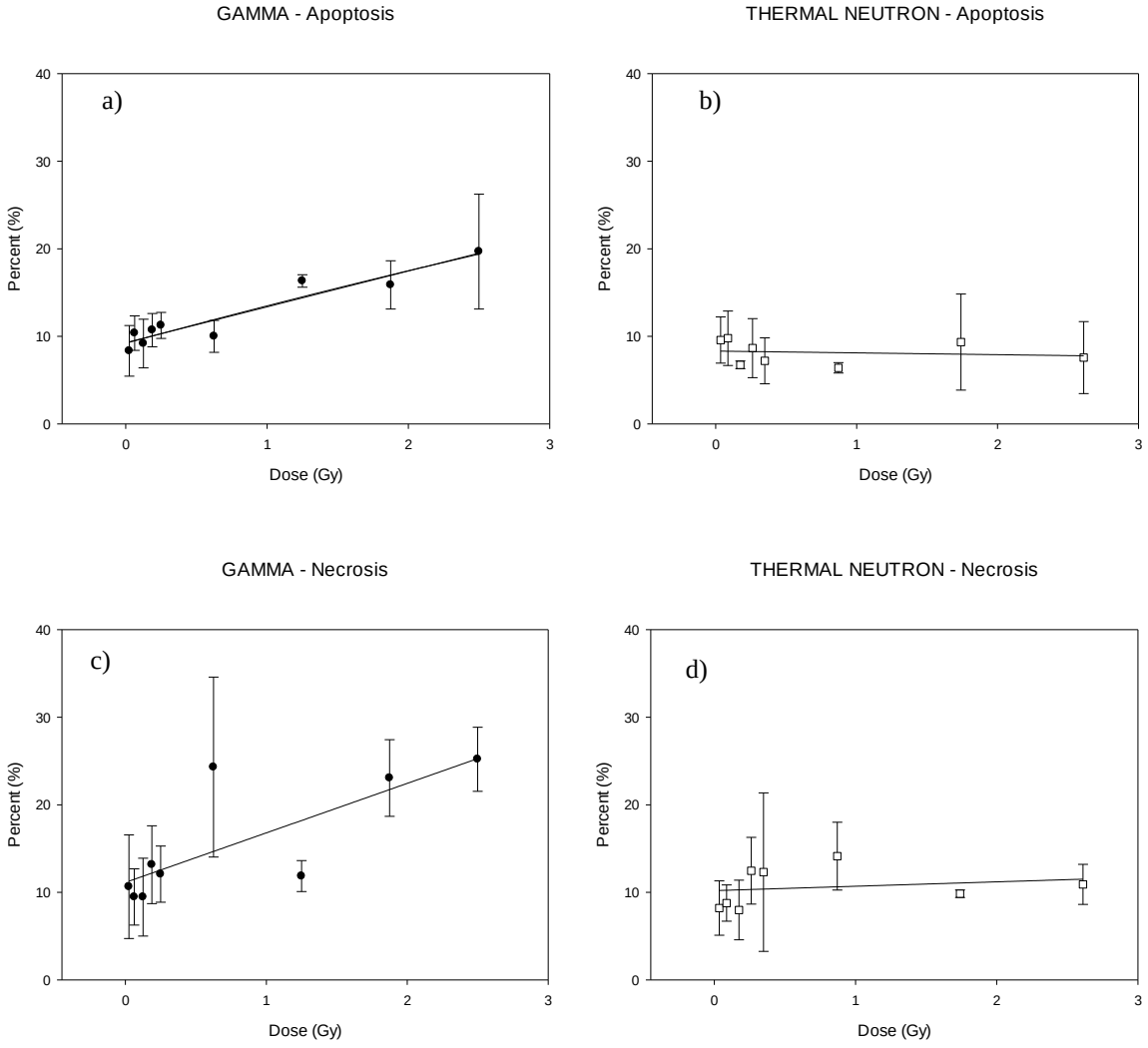

Figure 3: Percentage of apoptosis versus dose for gamma rays (a) and thermal neutrons (b). Percentage of necrosis versus dose for gamma rays (c) and thermal neutrons (d). Error bars represent standard error.

It was assumed that the behaviour of lymphocytes following irradiation is constant across donors. Percent apoptosis and necrosis was calculated for each donor. The mean and standard error is reported in the above figures. The trend-line represents the linear best fit.

Figure 4 illustrates the percent cell death of the three control samples. These samples were included to ensure outside influences did not affect cell death. The controls did not show a significant elevation of either apoptosis or necrosis following their respective treatments.

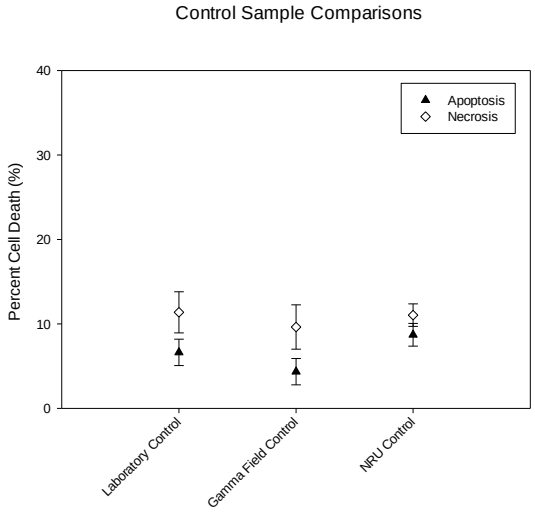

Figure 4: **Apoptosis and necrosis in control samples (0 Gy). Error bars represent standard error.**

3.2 Dicentric Chromosome Assay

Table 4 presents the raw chromosome data and Figure 5 demonstrates the linear relationship between aberrations per cell and dose. As both dicentric and centric ring chromosomes result from a minimum of two double strand breaks, this data has been summed and reported under the name "aberrations". Our preliminary data can be described by Equation (1) (R^2 of 0.86):

$$Ab = 0.2219D + 0.0045 \quad (1)$$

where Ab refers to aberrations per cell and D refers to dose (Gy).

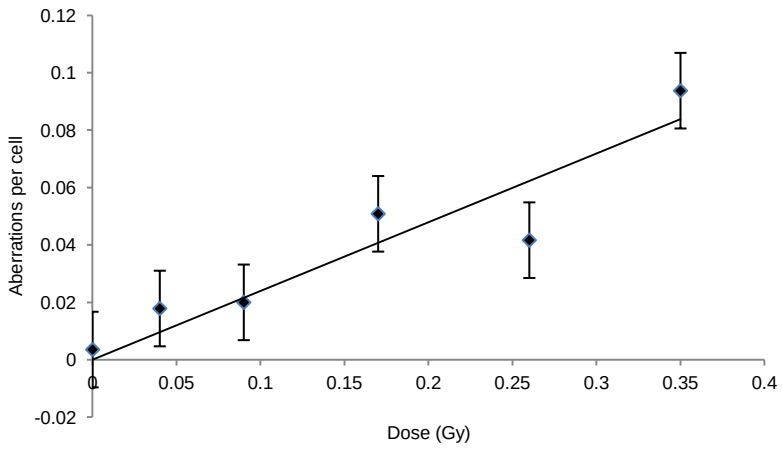

Figure 5: Aberrations per cell following thermal neutron exposure. Error bars represent standard error.

It is standard practice to test the results of the dicentric chromosome assay for compliance with the Poisson distribution. To achieve this, the dispersion index (ratio of the variance (σ^2) to the mean (y)) followed by the u test statistic (normalized unit of the dispersion index) is calculated. High-LET radiations typically produce over-dispersion (u values above 1.96 indicate over-dispersion at the 5% significance level), whereas low-LET radiations that comply to a Poisson distribution demonstrate u values that are near unity [24]. Our data set conforms to the Poisson distribution at all but one dose point (0.17 Gy) (Table 4). This unexpected result is likely due to the very low doses and low metaphase numbers. Additional scoring is underway to further quantify dicentric and ring chromosome induction following higher thermal neutron doses.

Table 4: Distribution of chromosome aberrations following thermal neutron exposure

Dose (Gy)	Cells Scored	Aberrations	Distribution of aberrations			Aberrations (# cell^{-1})	Dispersion Index (σ^2/y)	u value
			0	1	2			
0.00	281	1	280	1	0	0.006	1.00	0
0.04	224	4	220	4	0	0.018	0.99	-0.16
0.09	200	4	196	4	0	0.020	0.98	-0.17
0.17	59	3	56	1	1	0.051	1.64	4.24
0.26	96	4	92	4	0	0.042	0.97	-0.25
0.35	64	6	58	6	0	0.094	0.92	-0.49

4. Discussion

The apoptotic and necrotic cell death data following gamma radiation exposure is in good agreement with the literature for doses of 1 Gy and higher [15, 26]. Unfortunately, there is no published data for gamma exposures below 1 Gy to use for benchmarking purposes. In contrast, a dose-response was not observed for either apoptosis or necrosis endpoints following thermal neutron exposure. Ryan et al. [13] began to see an increase of apoptosis at approximately 0.25 Gy (4.13 Sv) following 280 keV neutron exposure. Vral et al. [7] also noted an increase in apoptosis between 0.25 Gy and 0.50 Gy (2.80 Sv and 5.75 Sv, respectively) following 5.5 MeV

fast neutron exposure. In this work, even at the highest dose of 2.6 Gy (6.5 Sv), no significant increase in cell death was observed.

Given the lack of observed cell death following thermal neutron exposures, we initially considered that not enough thermal neutron dose was being delivered to the blood volumes in order to achieve cell death. However, the dicentric chromosome assay data illustrated in Figure 5 indicates a linear dose response with a slope similar to that published by Schmid et al. (2013) [8]. With that said, in our work, it was assumed that the nitrogen content of the blood was 2.9%. This value was incorporated into MCNP5 to obtain the dose conversion coefficient of 0.231pGy cm^2. Sodium citrate anticoagulant comprised approximately 10% of the final blood volume and therefore, the nitrogen concentration in the irradiated blood samples would have been slightly less than the 2.9% modeled. This small reduction in nitrogen concentration would have slightly reduced the doses delivered and this may have had an impact on the level of cell death seen. We are currently investigating techniques to quantify nitrogen content to better refine our model.

We previously stated that the $^{14}N(n,p)^{14}C$ reaction is the primary mechanism responsible for dose delivery. This conclusion is reinforced in the experimental data. Specifically, even though the CNBC thermal neutron beam is contaminated with a small amount of low-LET radiation, experimental controls placed inside the gamma field, but outside the thermal neutron beam, showed no increase in chromosome aberrations or cell death compared to background. This also is in agreement with the findings of Schmid et al. (2013) who had 24% low-LET radiation contamination and did not see an increase in chromosome aberrations [11].

Unfortunately, with the available experimental data to date, it is currently unclear why thermal neutrons are able to induce chromosome aberrations but are unable to cause significant cell death. It is understood that thermal neutrons affect biological systems via absorption reactions whereas fast neutrons can impart dose via scattering reactions. These interaction differences may affect cellular behaviour post-irradiation and could possibly account for the results observed following fast neutron exposures [5,6]. It is also possible that the experimental timings did not allow for the full development of a cell death response. This possibility is currently being explored, however, this is in direct contrast to higher-energy neutron cell death experiments that demonstrated a cell death response at 24-96 hours [7, 13].

5. Conclusion

This paper examined apoptosis and necrosis in human peripheral blood lymphocytes following thermal neutron and ^{60}Co gamma exposures. It was determined that there is no correlation between thermal neutron dose and cell death. In contrast, a dose-response was observed for gamma radiation. While more work needs to be completed, cell death assays may provide a method for determining radiation quality and absorbed dose following unknown exposures. It is important to put future effort into understanding these surprising results.

6. Acknowledgements

This project formed part of AECL's Federal S&T program. The authors would like to acknowledge S. Pecoskie for his technical assistance and R. McGirl, A. Klein, and Y. Mullin for performing routine phlebotomy throughout this project (often with very little notice).

7. References

[1] J. F. Kerr, A. H. Wyllie, and A. R. Currie, "Apoptosis: a basic biological phenomenon with wide-ranging implications in tissue kinetics," *Br J Cancer,* vol. 26, pp. 239-57, Aug 1972.

[2] N. Shinomiya, "New concepts in radiation-induced apoptosis: 'premitotic apoptosis' and 'postmitotic apoptosis'," *Journal of Cellular and Molecular Medicine,* vol. 5, pp. 240-253, Jul-Sep 2001.

[3] M. Verheij and H. Bartelink, "Radiation-induced apoptosis," *Cell Tissue Res,* vol. 301, pp. 133-42, Jul 2000.

[4] V. A. Fadok, D. R. Voelker, P. A. Campbell, J. J. Cohen, D. L. Bratton, and P. M. Henson, "Exposure of phosphatidylserine on the surface of apoptotic lymphocytes triggers specific recognition and removal by macrophages," *J Immunol,* vol. 148, pp. 2207-16, Apr 1 1992.

[5] J. I. Hitomi, D. E. Christofferson, A. Ng, J. H. Yao, A. Degterev, R. J. Xavier, *et al.*, "Identification of a Molecular Signaling Network that Regulates a Cellular Necrotic Cell Death Pathway," *Cell,* vol. 135, pp. 1311-1323, Dec 26 2008.

[6] D. Hanahan and R. A. Weinberg, "Hallmarks of Cancer: The Next Generation," *Cell,* vol. 144, pp. 646-674, Mar 4 2011.

[7] A. Vral, M. Cornelissen, H. Thierens, H. Louagie, J. Philippe, K. Strijckmans, *et al.*, "Apoptosis induced by fast neutrons versus 60Co gamma-rays in human peripheral blood lymphocytes," *Int J Radiat Biol,* vol. 73, pp. 289-95, Mar 1998.

[8] E. Schmid, D. Regulla, S. Guldbakke, D. Schlegel, and M. Roos, "Relative biological effectiveness of 144 keV neutrons in producing dicentric chromosomes in human lymphocytes compared with 60Co gamma rays under head-to-head conditions," *Radiat Res,* vol. 157, pp. 453-60, Apr 2002.

[9] E. Schmid, D. Regulla, S. Guldbakke, D. Schlegel, and M. Bauchinger, "The effectiveness of monoenergetic neutrons at 565 keV in producing dicentric chromosomes in human lymphocytes at low doses," *Radiation Research,* vol. 154, pp. 307-312, Sep 2000.

[10] E. Schmid, D. Schlegel, S. Guldbakke, R. P. Kapsch, and D. Regulla, "RBE of nearly monoenergetic neutrons at energies of 36 keV-14.6 MeV for induction of dicentrics in human lymphocytes," *Radiation and Environmental Biophysics,* vol. 42, pp. 87-94, Jul 2003.

[11] E. Schmid, F. M. Wagner, L. Canella, H. Romm, and T. E. Schmid, "RBE of thermal neutrons for induction of chromosome aberrations in human lymphocytes," *Radiat Environ Biophys,* vol. 52, pp. 113-21, Mar 2013.

[12] K. Tanaka, N. Gajendiran, S. Endo, K. Komatsu, M. Hoshi, and N. Kamada, "Neutron energy-dependent initial DNA damage and chromosomal exchange," *J Radiat Res,* vol. 40 Suppl, pp. 36-44, Dec 1999.

[13] L. A. Ryan, R. C. Wilkins, N. M. McFarlane, M. M. Sung, J. P. McNamee, and D. R. Boreham, "Relative biological effectiveness of 280 keV neutrons for apoptosis in human lymphocytes," *Health Phys*, vol. 91, pp. 68-75, Jul 2006.
[14] R. Nolte, K. H. Muhlbradt, J. P. Meulders, G. Stephan, M. Haney, and E. Schmid, "RBE of quasi-monoenergetic 60 MeV neutron radiation for induction of dicentric chromosomes in human lymphocytes," *Radiat Environ Biophys*, vol. 44, pp. 201-9, Dec 2005.
[15] R. C. Wilkins, B. C. Kutzner, M. Truong, J. Sanchez-Dardon, and J. R. N. McLean, "Analysis of radiation-induced apoptosis in human lymphocytes: Flow cytometry using Annexin V and propidium iodide versus the neutral comet assay," *Cytometry*, vol. 48, pp. 14-19, May 1 2002.
[16] A. E. Meijer, U. S. Kronqvist, R. Lewensohn, and M. Harms-Ringdahl, "RBE for the induction of apoptosis in human peripheral lymphocytes exposed in vitro to high-LET radiation generated by accelerated nitrogen ions," *Int J Radiat Biol*, vol. 73, pp. 169-77, Feb 1998.
[17] D. T. Goodhead, "Spatial and temporal distribution of energy," *Health Phys*, vol. 55, pp. 231-40, Aug 1988.
[18] MCNP, "MCNP - A General Monte Carlo N-Particle Transport Code, Version 5," Los Alamos National Laboratory, Los Alamos2008.
[19] ICRP, "Report on the Task Group on Reference Man. ICRP Publication 23," *Annals of the ICRP*, vol. 23, 1975.
[20] W. G. Cross and H. Ing, "Conversion and Quality Factors Relating Neutron Fluence and Dosimetric Quantities," *Radiation Protection Dosimetry*, vol. 10, pp. 29-42, 1985.
[21] H. A. Bethe, "The Range-Energy Relation for Slow Alpha-Particles and Protons in Air," *Reviews of Modern Physics*, vol. 22, pp. 213-219, 1950.
[22] L. C. Northcliffe and R. F. Schilling, "Range and stopping-power tables for heavy ions," *Atomic Data and Nuclear Data Tables*, vol. 7, pp. 233-463, 1970.
[23] ICRP, *Basic Anatomical and Physiological Data for Use in Radiological Protection Reference Values. ICRP Publication 89* vol. 32 (3-4), 2002.
[24] IAEA, *Cytogenetic Dosimetry: Applications in Preparedness for and Response to Radiation Emergencies*. Vienna: IAEA, 2011.
[25] K. Kurosaka, M. Takahashi, N. Watanabe, and Y. Kobayashi, "Silent cleanup of very early apoptotic cells by macrophages," *Journal of Immunology*, vol. 171, pp. 4672-4679, Nov 1 2003.
[26] T. J. Liegler, W. Hyun, T. S. Yen, and D. P. Stites, "Detection and quantification of live, apoptotic, and necrotic human peripheral lymphocytes by single-laser flow cytometry," *Clin Diagn Lab Immunol*, vol. 2, pp. 369-76, May 1995.